

Surface roughness-controlled superelastic hysteresis in shape memory microwires

Stian M. Ueland, Christopher A. Schuh¹

*Department of Materials Science and Engineering, Massachusetts Institute of Technology,
77 Massachusetts Avenue, Cambridge, MA 02139, USA*

Superelasticity in Cu-Zn-Al shape memory alloy microwires is studied as a function of surface roughness. Wires with a rough surface finish dissipate more than twice as much energy per unit volume during a superelastic cycle than do electropolished wires with smooth surfaces. We attribute the increased damping in wires with large surface roughness to the increased density of surface obstacles where frictional energy is dissipated as heat during martensitic phase transformation.

Keywords: shape memory alloys (SMA); atomic force microscopy (AFM); damping; drawing; fibers

¹ Corresponding author. Email address: schuh@mit.edu (C.A Schuh).

Fine wires of Cu-based shape memory alloys (SMAs) with bamboo grain structure are interesting because they exhibit single crystal-like behavior without the restrictions in size and cost that come with single crystal production [1]. Recent interest in these structures, which typically have diameters below $\sim 100 \mu\text{m}$, has revealed several size effects upon the martensitic transformation, such as a transition from multi-domain to single-domain martensite morphology [2] and an increased hysteresis size in smaller wires [3]. These effects have been ascribed to two related phenomena. First, there is a transition from volume-obstacle control to surface-obstacle control of the martensitic phase transformation at wire diameters below about $\sim 100 \mu\text{m}$ [2, 4]. Secondly, below $100 \mu\text{m}$ in the regime of surface-obstacle control, the sampling of obstacles at the wire surface scales with surface-to-volume ratio, i.e., as the reciprocal of the wire diameter [2].

In the surface-obstacle control regime ($< 100 \mu\text{m}$), the condition of the surface of an SMA should be expected to have a major effect on its properties. Previous investigations on surface roughness in SMAs, however, have been on bulk samples. These include studies on fatigue [5], corrosion [6], surface chemistry [7], and due to the use of shape memory materials in medical devices, interactions with cells [8, 9]. Still using millimeter size samples, Chmielus et al. investigated the forward transformation in Ni-Mn-Ga [10]. They found that polished samples showed serrated stress-strain curves, while those of unpolished samples were smooth, and that polished samples exhibited lower twinning stress [10, 11]. Meanwhile, hysteresis size and shape depend on factors such as grain size [12], phase compatibility [13] and second phase particles [14, 15].

All of the above studies were conducted on “bulk” samples where the surface can be expected to play only a minor role on mechanical properties. It is the objective of this work to study the correlation between surface roughness and the width and shape of the superelastic stress strain curve in Cu-Zn-Al microwires. We show that hysteresis is dramatically increased in wires with high surface roughness as compared to electropolished wires where the surface is smooth, providing a key validation of the notion of a “surface obstacle controlled” regime at sample size scales below about 100 μm .

Solid pieces of shape memory alloy with the composition Cu-22.9Zn-6.3Al (wt. %) were placed in an aluminosilicate glass tube that had a 4 mm inner diameter and a working temperature of ~ 1250 °C. The inside of the tube was subjected to low vacuum conditions and an oxy-acetylene burner was used to heat the glass/metal until the metal melted and the glass softened. The softened glass capillary, with molten metal at its core, was then drawn out of the hot zone, reducing its diameter and hardening it. Fig. 1a shows an optical micrograph of such a glass-coated metallic fiber after drawing. The fibers were annealed at 800 °C in an argon atmosphere for 3 h and water quenched; during annealing the grains grow to span the wire cross section, forming a bamboo grain structure [16]. After annealing, the glass coating was removed by immersion in ~ 10 % diluted aqueous hydrofluoric acid. Fig. 1b shows a scanning electron micrograph of a wire after glass removal. The surface is observed to be rather rough with features reminiscent of valleys running parallel to the wire axis. Finally, the wires were electropolished at room temperature in an electrolyte consisting of 67 % phosphoric acid and 33 % deionized water for 30-120 s depending on wire size. The electrolyte was stirred at 80 rpm, the electrodes were pure Cu and

the polishing voltage was 2.8 V. Fig. 1c shows a scanning electron micrograph of a representative wire after electropolishing. The rough features of the as-drawn wire are removed; the surface is smooth and the wire diameter is uniform. Differential scanning calorimetry (DSC) of a polished wire with diameter 65 μm (not shown) revealed the transformation temperatures to be $A_f \sim 25$, $A_s \sim 9$, $M_s \sim 8$ and $M_f \sim -6$ $^\circ\text{C}$.

Fig. 2 shows atomic force microscopy (AFM) topography images of an unpolished and a polished wire. As in the micrograph in Fig. 1b, valleys running parallel to the wire axis characterize the unpolished wire. The polished wire in Fig. 2b shows a smooth surface, much like the micrograph in Fig. 1c, where the roughness associated with processing is removed. To obtain quantitative measures of surface roughness we determine the commonly used parameters R_q and R_a , calculated after subtracting the wire curvature using a first order flattening. The root mean square surface roughness parameter R_q was found to be 10 and 125 nm for the polished and unpolished wires, respectively. Similarly, the arithmetic average roughness parameter R_a was calculated to be 7 and 88 nm for the polished and unpolished wires, respectively. For comparison, the surface roughness parameter R_a in commercial Ni-Ti wire was found to lie between 23 and 281 nm [17] and between 100 and 350 nm in orthodontic wires [18].

To investigate the role of surface roughness on superelasticity we cut one of the as-drawn wires in two parts and electropolished one of the halves, but not the other. The diameter of the unpolished wire (rough surface) was 80 μm and that of the polished

wire (smooth surface) was 41 μm , due to the removal of surface layers. These two wires were then tested in tension at 35 $^{\circ}\text{C}$ in a dynamic mechanical analyzer (DMA Q800 from TA instruments) operated in load control at a loading rate of 10 $\text{MPa}\cdot\text{min}^{-1}$ during transformation. The gauge lengths were 8.2 and 5 mm for the polished and unpolished wires, respectively.

Fig. 3a shows superelastic stress strain curves of the rough and smooth wires for the first cycle (not previously deformed). The slopes of the transformation plateaus are similar (~ 600 MPa) but the forward plateau is at a higher stress and the reverse plateau is at a lower stress for the rough wire compared to the smooth wire. The stress to induce martensite is about 26 and 20 MPa for the rough and the smooth wires, respectively, and the rough wire shows a much larger hysteresis size than the polished wire. The strain-averaged vertical hysteresis sizes are 21.5 and 8.5 MPa for the rough and polished wires, respectively; the energy dissipation of the two wires differ by a factor of 2.5.

The properties of Cu-Zn-Al and many other SMAs evolve with cycling before they reach a somewhat stable response after about ten cycles [1]. Fig. 3b shows the superelastic curves from the tenth cycle where the curves have reached a steady state [1]. Interestingly, the forward plateaus are now similar, however, the difference between the two reverse plateaus is still large. In fact, their energy dissipation still differs by a factor of 2.5 (hysteresis sizes are now 11.3 and 4.7 MPa for the rough and the polished samples).

We estimate that the gauge sections of these two wires sample about 40 and 65 grains (rough and polished wires, respectively) and we therefore believe that factors such as grain size and orientation play only minor roles in affecting SMA properties [16]. Furthermore, since both samples were cut from the same wire, composition and internal microstructure, e.g. dislocation density, are assumed to be similar. Lastly, previous studies have shown that smaller wires in this size range exhibit larger hysteresis than larger wires [3]. In a previous paper we ascribed this size effect to the increased sampling of obstacles at the wire surface by the austenite/martensite interface [2]. Thus, it is especially suggestive that although the diameter of the polished wire in Fig. 3 is finer (due to removal of surface layers by electropolishing), this sample still dissipates less energy per unit volume than does the rough wire. After ruling out microstructural and compositional differences as well as size effects, we are left to conclude that the difference in hysteresis between the two wires is attributable to the difference in surface roughness.

In SMAs, frictional energy is dissipated as heat when the austenite/martensite interface moves past obstacles. In line with this, hysteresis size has been shown to decrease with increasing degree of crystal perfection [19]. In small scale SMAs, the sampling of obstacles at the wire surface has been put forward as the dominant source of energy damping [2]; as noted in the introduction, the scaling of hysteresis with wire diameter aligns with this proposal for wires below about 100 μm in size scale. Because electropolishing reduces surface roughness it appears reasonable to assume that it reduces both the amount as well as the ‘frictional potential’ of obstacles at the

surface. Based on the above we interpret the results of Fig. 3 in the following way: the smoother the wire surface, the fewer obstacles there are, and because fewer (and less potent) obstacles are bypassed by the moving austenite/martensite interface less energy is dissipated during a superelastic cycle. To demonstrate the generality of the observations from Fig. 3 we now show data from superelastic curves for several polished and unpolished wires. In Fig. 4 we plot the strain-averaged vertical hysteresis size for wires with a range of diameters. The general trend is observed to be the same as for the wire presented above: wires with a smooth, polished surface dissipate less energy than wires with rough surfaces. Furthermore, many of the polished wires show a hysteresis size of about 5-10 MPa, which is similar to single crystalline bulk samples of Cu-Zn-Al [20]. This means that even though the wires are in a size range where properties have been shown to be surface-controlled [2], electropolishing mitigates this effect by removing surface obstacles. On the other hand, some of the polished wires show a hysteresis size comparable to the rough wires and these wires are in the lower end of the diameter range studied. These outliers may suggest that electropolishing simply translates the size effect in damping to a smaller scale, not well captured in the present study. In line with this, submicron Cu-Al-Ni pillars show increased damping, despite having smooth surfaces [21].

The present results are not only scientifically interesting for their implications on surface effects upon the martensitic transformation, but also have important practical implications. For example, high damping is desired in many applications, such as impact absorption [22], but unwanted in others, such as actuation and energy harvesting [13]. The ability to tailor the degree of damping by simply controlling

surface roughness could in principle be useful, especially as SMAs find use in structures with large surface areas [23].

In summary we show that energy dissipation in Cu-Zn-Al microwires may be tuned by controlling surface roughness. This provides experimental evidence of the relation between hysteresis size and obstacle density/potency, especially in the fine scale (< 100 μm) where properties in SMA structures have been proposed to be surface-controlled.

Acknowledgements - This work was supported by the US Office of Army Research, through the Institute for Soldier Nanotechnologies at MIT.

- [1] Ueland SM, Schuh CA. *Acta Mater* 2012;60:282.
- [2] Ueland SM, Schuh CA. *Acta Mater* 2013;61:5618.
- [3] Ueland SM, Chen Y, Schuh CA. *Adv Funct Mater* 2012;22:2094.
- [4] Chen Y, Schuh CA. *Acta Mater* 2011;59:537.
- [5] Chan CW, Man HC, Cheng FT. *Mat Sci Eng a-Struct* 2013;559:407.
- [6] Milosev I, Kapun B. *Mat Sci Eng C-Mater* 2012;32:1087.
- [7] Armitage DA, Grant DM. *Mat Sci Eng a-Struct* 2003;349:89.
- [8] Li YC, Xiong JY, Wong CS, Hodgson PD, Wen C. *Tissue Eng Pt A* 2009;15:3151.
- [9] Cisse O, Savadogo O, Wu M, Yahia L. *J Biomed Mater Res* 2002;61:339.
- [10] Chmielus M, Rolfs K, Wimpory R, Reimers W, Mullner P, Schneider R. *Acta Mater* 2010;58:3952.
- [11] Chmielus M, Witherspoon C, Ullakko K, Mullner P, Schneider R. *Acta Mater* 2011;59:2948.
- [12] Kim M, Cho G, Noh J, Jeon Y, Kim Y, Miyazaki S, Nam T. *Scripta Mater* 2010;63:1001.
- [13] Delville R, Schryvers D, Zhang ZY, James RD. *Scripta Mater* 2009;60:293.
- [14] Hamilton RF, Sehitoglu H, Efstathiou C, Maier HJ. *Scripta Mater* 2007;57:497.
- [15] Bubani FD, Sade M, Lovey F. *Mat Sci Eng a-Struct* 2012;543:88.
- [16] Ueland SM, Schuh CA. *J. Appl. Phys.* 2013;114:053503.
- [17] Huang HH. *J Biomed Mater Res A* 2005;74A:629.

- [18] Pernier C, Grosgeat B, Ponsonnet L, Benay G, Lissac M. Eur J Orthodont 2005;27:72.
- [19] Van Humbeeck J, Kustov S. Smart Mater Struct 2005;14:S171.
- [20] Ortin J. J Appl Phys 1992;71:1454.
- [21] Juan JS, No ML, Schuh CA. Nat Nanotechnol 2009;4:415.
- [22] Karaca HE, Acar E, Basaran B, Noebe RD, Chumlyakov YI. Scripta Mater 2012;67:447.
- [23] Bhattacharya K, James RD. Science 2005;307:53.

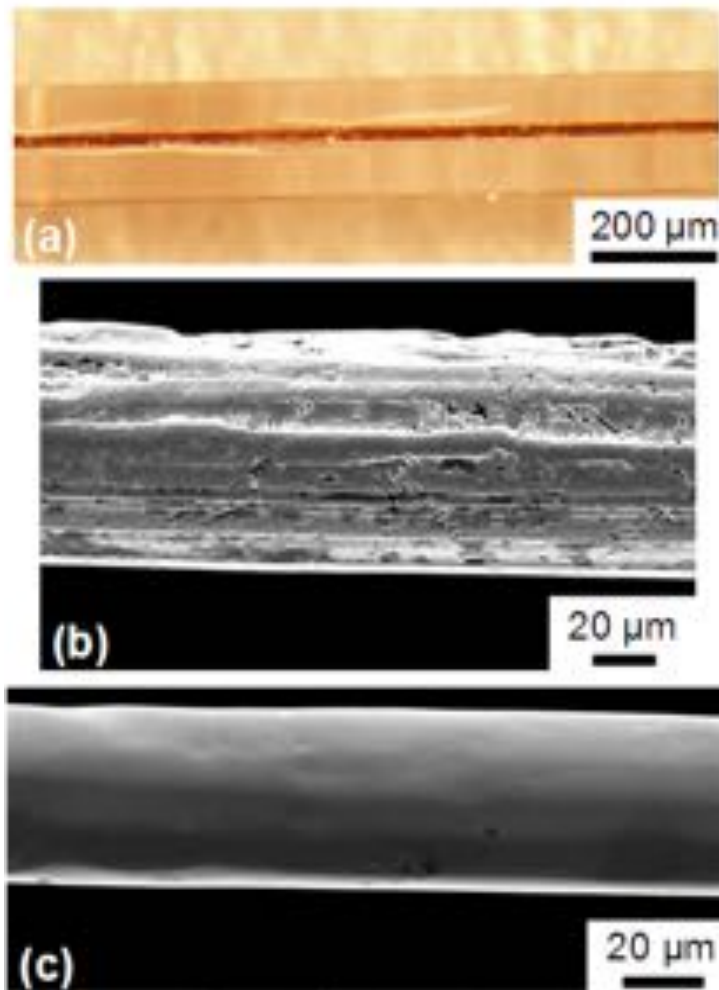


Figure 1. (a) Optical micrograph of an SMA wire inside its glass sheath after drawing, (b) scanning electron micrograph of the wire surface after glass removal and (c) scanning electron micrograph of a smooth wire surface after electropolishing.

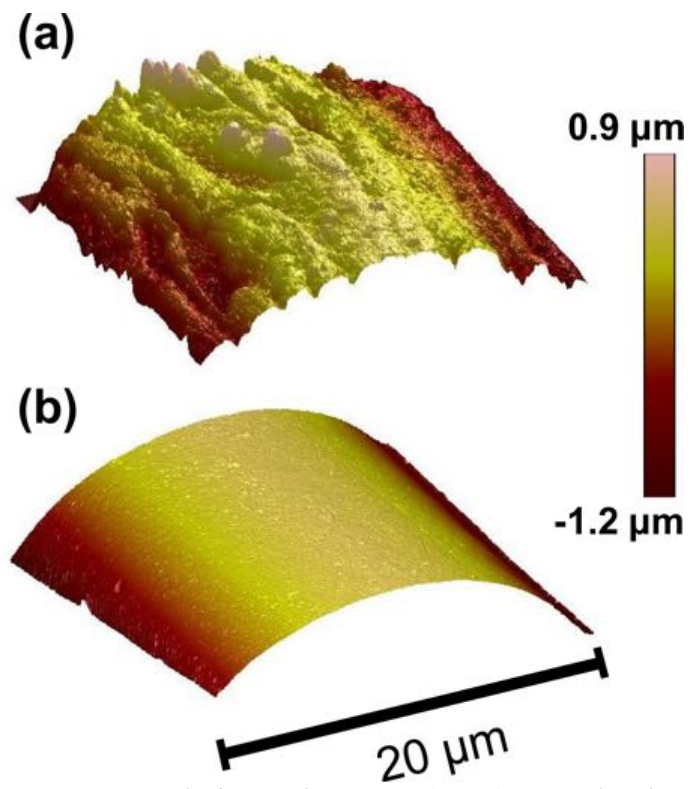


Figure 2. Atomic force microscopy (AFM) scans showing surface topography (a) before and (b) after electropolishing.

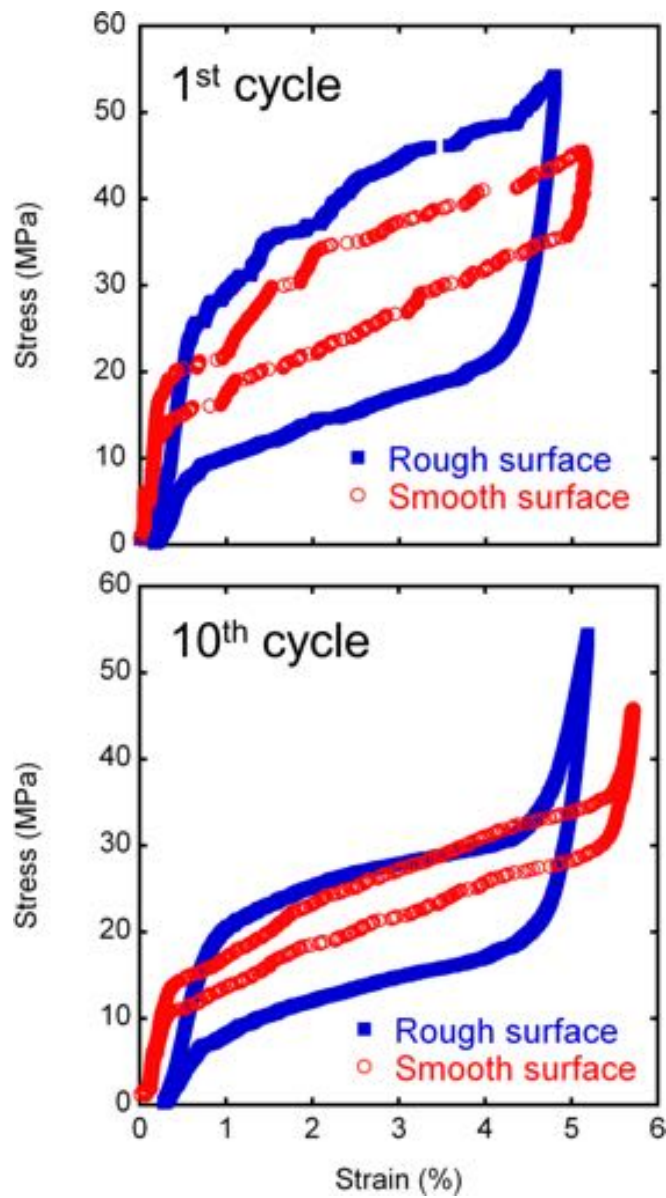


Figure 3. True stress-strain curves from the (a) first and (b) tenth cycle showing superelasticity of polished (open red circles) and not polished (solid blue squares) samples. Both samples were cut from the same initial wire segment and have diameters of 80 (unpolished) and 41 μm (polished).

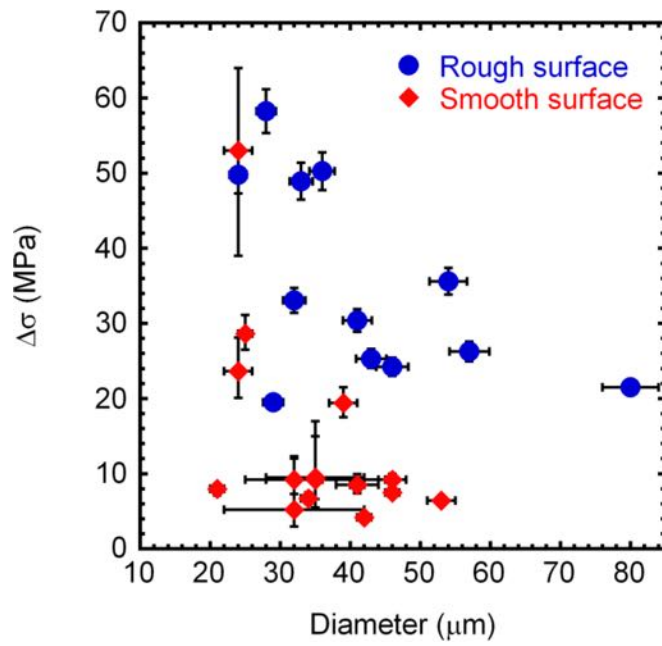


Figure 4. Strain-averaged hysteresis size in Cu-Zn-Al microwires plotted against wire diameter for polished and unpolished wires.